UNIFIED MODELLING OF TIG MICROARCS WITH EVAPORATION FROM COPPER ANODE

M. Baeva*, R.Methling, D. Uhrlandt

Leibniz Institute for Plasma Science and Technology, Felix-Hausdorff-Strasse 2, 17489 Greifswald, Germany

* baeva@inp-greifswald.de

Abstract. A previously developed unified model of a tungsten-inert gas (TIG) microarc has been extended to take into account the melting of the anode made of copper and the release of copper atoms due to its evaporation. The copper atoms enter the plasma to become excited and ionized. The presence of copper atoms and ions can strongly change the plasma parameters. The extended unified model further includes excited states of copper and collisional and radiative processes between them. Predictions of the parameters of the microarc plasma in the presence of copper species are presented and discussed.

Keywords: unified, non-equilibrium, modelling, microarc, metal vapour.

1. Introduction

Microarcs as scaled down but still powerful heat sources can represent alternatives to electron beams and lasers. They are applied for additive (re)manufacturing and material processing, e.g. in microarc welding, production of bioactive coatings. Microarcs are attractive objects for basic research, in which knowledge of the spatial structure of the arc is gained and evaluated for consideration in arc plasma models, which do not resolve the regions of space charge. A fluid model in atmospheric pressure argon [1] has been recently developed to provide a spatial resolution over the entire inter-electrode region, i.e. a unified non-equilibrium description of the microarc. The study of the microarc plasma carried out in the work [1] has been further extended to explore the potentials and limitations of one-dimensional in comparison to two-dimensional models [2] and the behaviour of the microarc plasma towards a minuscule discharge gap [3]. The present work considers the extension of the description that takes into account evaporation of the anode, which leads to the presence of metal vapour in the microarc plasma. We outline the extended chemistry and present results showing the influence of the metal vapour released from the melting anode on the plasma parameters. The predicted emission of metal atoms will enable comparisons with experimental findings.

2. Computational method

The computational model considers a parallel-plate configuration, including an anode made of copper and a ceriated tungsten cathode with a radius of $2\,\text{mm}$ and a length of $20\,\text{mm}$. The inter-electrode gap has a length of $400\,\mu\text{m}$ and contains argon at atmospheric pressure. The model is set up as one-dimensional (1D) in order to reduce the computational cost in making use of high level of plasma chemistry. It is based on the equations for conservation of species and energy, the Poisson equation for the electric potential, the heat transfer in the electrodes, and an electric circuit used to control the current density. Details of the model, except for the account for evaporation and the metal vapour in the plasma, have been given previously [1]. In what follows, we focus on the new features related to the presence of metal vapour. The features concerning the argon species remain the same as in reference [1].

The unified model of the microarc employs a fluid description that involves electron, ground state atoms and ions of argon and copper, a group of excited argon atoms (4s, 4p), excited levels of copper $4\text{s}^2\ ^2\text{D}_{5/2}$, $4\text{s}^2\ ^2\text{D}_{3/2}$, $4^2\text{P}_{1/2}$, $4^2\text{P}_{3/2}$, and groups of excited levels ($^4\text{P}^0$, $^4\text{D}^0$, $^4\text{F}^0$), ($5^2\text{P}_{1/2}$, $5^2\text{P}_{3/2}$, $4^2\text{D}_{3/2}$, $4^2\text{D}_{5/2}$) according to [4]. Doubly charged copper ions are not included in the model, since the second ionization potential of copper of $20.29\,\text{eV}$ lies quite above the first ionization potential of argon. The cross sections for electron impact excitation and ionization, and rate coefficients for collisions between species of argon and copper are taken from [4] and the references therein. 11 radiative transitions between copper states are taken into account. A self-absorption for the resonance transitions at $324.7\,\text{nm}$ and $327.4\,\text{nm}$ is taken into account in terms of space-independent effective lifetimes [5]. All other transitions are treated as optically thin.

The heavy species are in equilibrium at a common temperature T while the electrons are described assuming a Maxwellian velocity distribution at a temperature T_e. The unified model implies the drift-diffusion approximation in the description of the electron transport. It solves the equations for conservation of species and energy of electrons and heavy particles, the Poisson equation for the self-consistent electric field, the heat transfer in the electrodes. The control of the density of electric current is realized by considering

an external electric circuit with a ballast resistor and a voltage source. Gas flow and self-induced magnetic field are not considered for low currents.

The boundary conditions to the microarc model concerning the plasma and the cathode are those reported in [1]. While in previous works a fixed temperature of 300 K is set on the plasma edge to the anode, here we consider the anode as a cylindrical rod made of copper, whose length of 100 mm is much larger than its radius of 2 mm and we solve the heat transfer in the anode body. In the case of no volume source (Joule heating is neglected since the current is low) the equation reads

$$A_s\rho C_p\frac{\partial T}{\partial t} + \nabla\cdot\mathbf{q}_s = 0. \tag{1}$$

In Equation (1), A_s is the cross section area of the anode, ρ is the mass density, and C_p is the specific heat capacity at constant pressure of the anode material. $\mathbf{q}_s = -A_s\kappa\nabla T$ is the heat flux due to heat conduction and κ is the heat conductivity of the material. Considering the model in 1D along the axis x, the boundary condition of Eq. (1) at the end, which is not in contact with the plasma, is set as T=300 K. The the boundary condition on the side with contact to the plasma is written as

$$\kappa\frac{\mathrm{d}T}{\mathrm{d}x} = q_a - \mathcal{L}J_{\mathrm{vap}}m_{\mathrm{v}}. \tag{2}$$

On the r.h.s. in Eq. (2), the first term q_a denotes the heat flux from the plasma, the second term describes the heat loss due to evaporation with J_{vap} being the flux of evaporated copper atoms with a mass m_{Cu}. Similarly to the heat flux from the plasma to the cathode given in [1], the flux q_a is written as

$$q_a = j_{i,\mathrm{Ar}^+}(E_{\mathrm{ion,Ar}} - \Phi_{\mathrm{Cu}}) + j_{i,\mathrm{Cu}^+}(E_{\mathrm{ion,Cu}} - \Phi_{\mathrm{Cu}})$$
$$+ \frac{1}{4}n_e v_{th,e}(2k_B T_e + e\Phi_{\mathrm{Cu}}) - \epsilon_{\mathrm{Cu}}\sigma_{\mathrm{SB}}T_{\mathrm{w}}^4 \tag{3}$$

and accounts for recombination of singly charged ions of argon and copper, a flux of electrons from the plasma and their condensation in the anode, and a black-body radiation. j_{i,Ar^+} and j_{i,Cu^+} are the ion current densities of respectively argon and copper ions, $E_{\mathrm{ion,Ar}}$ and $E_{\mathrm{ion,Cu}}$ are the corresponding ionization potentials, Φ_{Cu} – the work function of copper ($E_{\mathrm{ion,Ar}}$, $E_{\mathrm{ion,Cu}}$ and Φ_{Cu} are expressed in units of Volt), k_B – the Boltzmann constant, e is the elementary charge, σ_{SB} - the Stefan-Boltzmann constant, and ϵ_{Cu} – the emissivity of copper.

The flux J_{vap} is obtained applying the Langmuir equation [6]

$$J_{\mathrm{vap}} = p_{\mathrm{Cu}}/\sqrt{2\pi m_{\mathrm{Cu}}k_B T_{\mathrm{w}}}, \tag{4}$$

in which p_{Cu} denotes the equilibrium pressure of the metal vapour at temperature of the wall T_{w}.

$$p_{\mathrm{Cu}} = 133.3[Pa]T_{\mathrm{w}}^{-1.27}10^{13.39-17656/T_{\mathrm{w}}}. \tag{5}$$

The latent heat of evaporation $\mathcal{L}$ is expressed through the boiling T_{b} and critical T_{c} temperatures [6]:
$$\mathcal{L} = \begin{cases} \mathcal{L}_0(T_{\mathrm{c}} - T_{\mathrm{w}})/(T_{\mathrm{c}} - T_{\mathrm{b}}) & \text{if } T_{\mathrm{w}} > T_{\mathrm{b}} \\ \mathcal{L}_0 & \text{if } T_{\mathrm{w}} \leq T_{\mathrm{b}} \end{cases}$$
with $\mathcal{L}_0$=4.73 MJ/kg, T_{b}=2868 K, T_{c}=5421 K.

Provided the temperature for melting T_{m}=1356 K is reached, the anode material undergoes a phase change. The latter is accounted for in solving Eq.(1) by means of the method of apparent heat capacity. According to this method, a phase transition function $\alpha(T)$ is introduced to enable a smooth transition between the solid and liquid phases within a given interval ΔT around the temperature of phase transition T_m. The heat capacity of the two phases in this interval is expressed as $C_p = C_{p,s}(1 - \alpha) + C_{p,l}\alpha$. For the solid we set $\alpha = 0$ and for the liquid $\alpha = 1$. The latent heat of fusion H_{f} is further included as an additional term to C_p, i.e. C_p reads

$$C_p = C_{p,s}(1 - \alpha) + C_{p,l}\alpha + H_{\mathrm{f}}\frac{\mathrm{d}\alpha}{\mathrm{d}T}. \tag{6}$$

When copper vapour can be released from the anode, the mass flux $J_{\mathrm{vap}}m_{\mathrm{v}}$ serves as a boundary condition for the equation describing the transport of ground state copper atoms, which are excited and ionized, and undergo collisions with argon species.

3. Results and discussion

When the anode is kept at constant temperature of 300 K, the microarc plasma contains only species of argon. The plasma properties of a microarc with a length of 400 µ m in pure argon have been analyzed in a previous work [3].

Figure 1 shows the predicted temperature, T_a, on the anode end, which is in contact with the plasma and the voltage V_{arc} for several values of the current density. Additional lines mark the levels corresponding to the melting (T_{m}) and boiling (T_{b}) temperatures. The T_a-values obtained for current densities between 3×10^5 and 5.8×10^5 A/m^2 are located between the marked levels so that copper atoms released from the anode are expected to influence the plasma parameters. For example, the microarc voltage V_{arc} increases in comparison to the case of a cooled anode (shown as solid symbols) for the T_a values presented in Fig. 1.

Figure 2 shows the distribution of the gas temperature T and the electron temperature T_e in the discharge gap. Distance $x = 0$ corresponds to the position of the anode, while the cathode is at $x = 400$ µm. The electron temperature is presented for x from 380 µm up to 400 µm (see the scale on the top of the graph) in order to enlarge the peak in the cathode space charge sheath. The results are obtained at current density of about 5.8×10^5 A/m^2. When the anode is not cooled, the gas temperature on the anode side increases, while it decreases in the remaining part of the arc column. The electron temperature in the
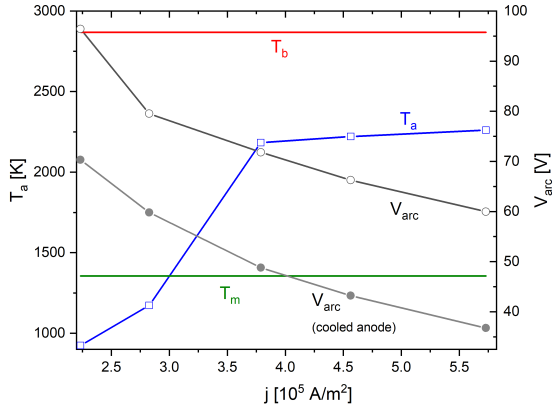
Figure 1. Temperature on the anode surface T_a and arc voltage V_{arc} versus current density. Solid symbols correspond to the case of cooled cathode (pure argon plasma).
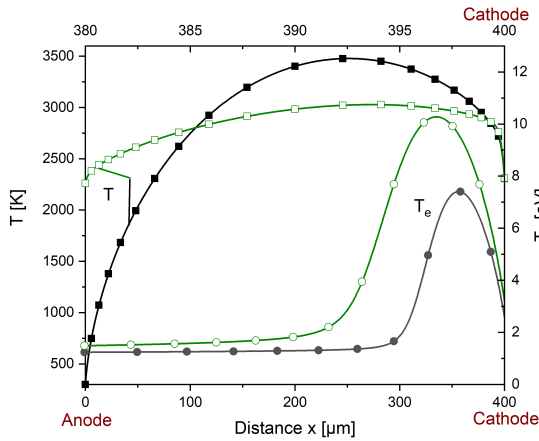

Figure 2. Gas temperature T (squares) and electron temperature T_e (circles) for current density 5.8×10^5 A/m^2. Solid symbols correspond to the case of cooled cathode (pure argon plasma).

Figure 3. Species number densities for current density 5.8×10^5 A/m^2: electrons n_e (squares), ions n_{Ar^+} (circles), ions n_{Cu^+} (triangles), atoms n_{Cu} (diamonds). Solid symbols correspond to the case of cooled cathode (pure argon plasma).

Figure 4. Ratios of atom number densities n_{Cu}/n_{Ar} (solid symbols and scale on the left side) and ion number densities n_{Cu^+}/n_{Ar^+} (open symbols and scale on the right side) for current density 5.8×10^5 A/m^2

cathode sheath significantly increases in comparison to pure argon plasma.

Figure 3 shows the predicted number densities of electrons, argon and copper ions, and copper atoms at a current density of 5.8×10^5 A/m^2. In the case of pure argon plasma (cooled anode), the electron density n_e is balanced by the density of argon ions n_{Ar^+} in the quasineutral bulk of the microarc. When the anode is not cooled, the electron number density n_e increases in comparison to the value in pure argon plasma for distances from the anode up to about 50 µm. In this region, the quasineutrality in the plasma bulk is provided by the n_{Cu^+} number density. This effect can be explained with the strong production of copper atoms and their low ionization potential. The number density of argon ions n_{Ar^+} becomes progressively more noticeable towards the cathode. The profile of the electron density significantly changes in comparison to pure argon. Its values are lower by a factor above 2 in the middle of the gap. An increase of n_{Cu} in front of the cathode is observed, which is related to the recombination of copper ions and deactivation of ex-
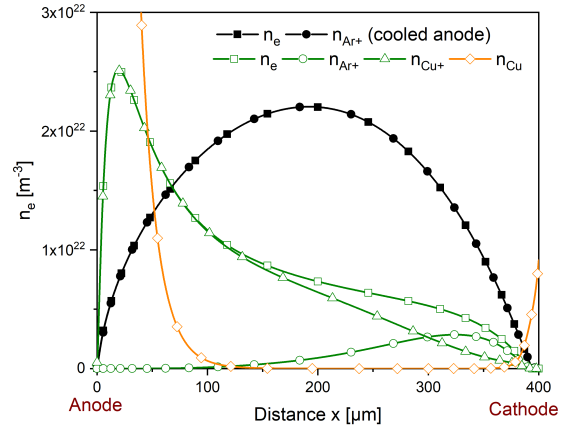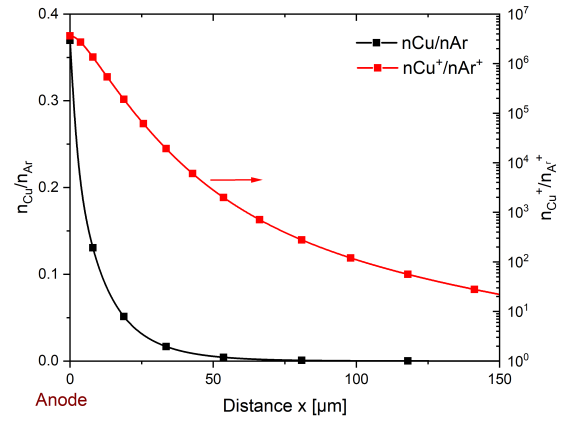
cited atoms on the cathode. Figure 4 shows the ratios of atom and ion densities, n_{Cu}/n_{Ar} and n_{Cu^+}/n_{Ar^+}, on the anode side of the microarc ($x < 150$ µm). We notice that n_{Cu}/n_{Ar} has a value of 0.37 at the anode and decreases rapidly to about 0.1 within a distance of 10 µm from the anode. However, the number density of copper ions exceeds that of argon ions over these distances by several orders of magnitude. This occurs due to the lower ionization potential of copper atoms (7.72 eV) in comparison with that of ground state argon atoms (15.76 eV). In addition, the excited copper atoms at and above level $4^2P_{1/2}$ with an ionization potential below 4 eV are easier ionized than the group of excited states of argon.

Estimates of the thickness of the space-charge sheaths adjacent to the anode and the cathode are performed according to the definition by Tonks and Langmuir. The edge between the quasineutral bulk and the space-charge sheath is defined at the position x, where $(n_i - n_e)/n_i$=0.01. This gives at a current density of 5.7×10^5 A/m^2 a thickness of the anode
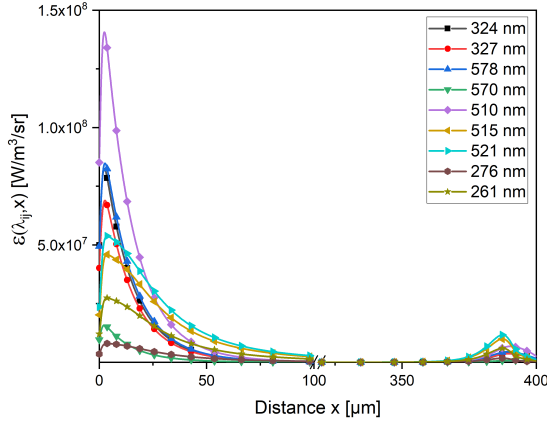
Figure 5. Spectral emission coefficient along the distance x for spectral lines of the copper atom considered in the model for a current density of 5.7×10⁵ A/m².

sheath of about 2.4 μm in pure argon and 1.26 μm in the presence of copper species. The thickness of the cathode space-charge sheath slightly increases to about 13 μm in presence of copper since the main influence of copper species is on the anode side of the microarc. However, the magnitude of the cathode fall increases by about 15 V if the anode is not cooled. This gives rise to the increase of the electron temperature (see Fig. 2). The anode fall becomes -2.55 V in the presence of copper instead of -4.3 V in pure argon.

Figure 5 presents the axial dependence of the spectral emission coefficient for spectral lines originating from excited states of Cu atoms considered in the model. The spectral emission coefficient is given as

$$\varepsilon(\lambda_{ij}, x) = \frac{1}{4\pi} \frac{hc}{\lambda_{ij}} A_{ij} n_i(x), \qquad (7)$$

where h is the Plank constant, c is the speed of light, A_{ij} is the probability of the radiative transition at wavelength λ_{ij} from level i to level j, and $n_i(x)$ is the number density of species on level i. The radiation from copper atoms occurs mostly close to the anode surface, where the electron density and copper atom density are largest (see Fig. 3). Then, the reaction rate for excitation of copper atoms, which is proportional to their product, becomes largest. A secondary increase appears in front of the cathode, which is related to the peak of the electron temperature (see Fig. 4).

Since the 1D model presumes that uniform plasma in radial direction, the values at a given distance x are proportional to the radial radiance that can be compared with results from "side-on" measurements. Such comparison has been done in a recent study on plasma between copper electrodes [7], where a good agreement of the model predictions and the experimental findings has been found.

The large length of the anode considered in the present model is beneficial for reaching temperatures beyond the melting point of copper and the release of copper metal vapour. In the practice, the thickness of the anode, whose back surface is kept at 300 K by

water-cooling, and the temperature on the plasma side are related. The maximum temperature reached on the plasma side increases with the anode thickness due to decrease of the temperature gradient. Model predictions can therefore be useful to obtain the onset of melting.

4. Conclusions

The thermal regime of the anode influences the parameters of the microarc plasma. The model presented predicts that a copper anode with a length of 100 mm and a radius of 2 mm melts for a current density beyond 3×10^5 A/m². The release of copper vapour into the plasma leads to a shift and an increase of the maximum electron and ion densities towards the anode. The evaporation of copper atoms progressively increases with the current density. For temperatures close to the boiling point, a noticeable amount of copper atoms and ions is predicted. Their influence is restricted to a distance from the anode, which is less than the half length of the gap.

References

[1] M. Baeva, D. Loffhagen, and D. Uhrlandt. Unified non-equilibrium modelling of tungsten-inert gas microarcs in atmospheric pressure argon. *Plasma Chem. Plasma Process.*, 39:949–968, 2019. doi:10.1007/s11090-019-10020-x.

[2] M. Baeva, D. Loffhagen, and D. Uhrlandt. Unified modelling of non-equilibrium microarcs in atmospheric pressure argon: potentials and limitations of one-dimensional models in comparison to two-dimensional models. *Japanese Journal of Applied Physics*, 59:SHHC05, 2020. doi:10.35848/1347-4065/ab71da.

[3] M. Baeva, D. Loffhagen, M. M. Becker, E. Siewert, and D. Uhrlandt. Plasma parameters of microarcs towards minuscule discharge gap. *Contrib. Plasma Phys.*, 60:e202000033, 2020. doi:10.1002/ctpp.202000033.

[4] A. Bogaerts, R. Gijbels, and R. Carman. Collisional - radiative model for the sputtered copper atoms and ions in a direct current argon glow discharge. *Spectrochimica Acta Part B*, 53:1679–1703, 1998. doi:10.1016/S0584-8547(98)00201-8.

[5] Y. Golubovskii, S. Gorchakov, D. Loffhagen, and D. Uhrlandt. Influence of the resonance radiation transport on plasma parameters. *Eur. Phys. J. Appl. Phys.*, 37:101–104, 2007. doi:10.1051/epjap:2006150.

[6] M. S. Benilov, S. Jacobsson, A. Kadani, and Z. S. Vaporization of a solid surface in an ambient gas. *J. Phys. D: Appl. Phys.*, 34:1993–1999, 2001. doi:10.1088/0022-3727/34/13/310.

[7] M. Baeva, V. F. Boretskij, D. Gonzalez, R. Methling, O. Murmantsev, D. Uhrlandt, and A. Veklich. Unified modelling of low-current short-length arcs between copper electrodes. *J. Phys. D: Appl. Phys.*, 54:025203, 2021. doi:10.1088/1361-6463/abba5d.